Four new trinuclear {$Cu_3(\mu_3\text{-}OH)(oximate)_3$}$^{2+}$ clusters: crystal structure and magnetic behaviour†

Saskia Speed,[*a] Mercè Font-Bardía,[b] M. Salah El Fallah[a] and Ramon Vicente[*a]

[a]Departament de Química Inorgànica, Universitat de Barcelona, Martí i Franquès 1-11, 08028 Barcelona, Spain.

E-mail: ramon.vicente@qi.ub.es, saskia.speed@qi.ub.es

[b]Departament de Cristal·lografia i Minerologia, Universitat de Barcelona, Martí i Franquès s/n, 08028 Barcelona, Spain

Four new triangular copper(II) complexes with the fragment {Cu3(μ3-OH)(oximate)3}2+ and formulae [Cu3(μ3-OH)(μ-Cl)(Py2CNO)3(tBuPO3H)]·4H2O (1), [Cu3(μ3-OH)(μ-Br)(Py2CNO)3(tBuPO3H)]·3.5H2O (2), [Cu3(μ3-OH)(μ-Br)(PhPyCNO)3(tBuPO3H)(MeOH)]·1.5 MeOH (3), [Cu3(μ3-OH)Cl2(PhPyCNO)3]·0.5H2O (4), (Py2CNO = di(2-pyridyl)ketoximate, PhPyCNO = phenyl(2-pyridyl)ketoximate, tBuPO3H2 = tert-butylphosphonic acid) are reported. The magnetic properties of compounds 1–4 were studied. The compounds were found to exhibit strong antiferromagnetic coupling and antisymmetric exchange interaction.

Introduction

The reaction of oximate ligands with paramagnetic 3d metal ions can generate polynuclear complexes with interesting magnetic properties, including single-molecule magnet behaviour.1–7 Among the polynuclear oximate compounds, a great number of isolated triangles with the {Cu3(μ3-OR)(oximate)3}n+ core have been well characterized.8–21 The magnetic response of these small molecules can be useful for determining the factors that influence the magnetic coupling and for studying the spin frustration phenomenon by testing the magnetic exchange models.22 The {Cu3(μ3-OR)(oximate)3}n+ core can be found also in discrete hexanuclear copper(II) cages with the [Cu3O···H···OCu3] motif.23–28

On the other hand, the phosphonate ligands can also generate polynuclear complexes with interesting magnetic properties, including single-molecule magnet behaviour.29 A possibility to explore can be to combine in the same synthesis oximate and phosphonate ligands with copper(II) salts to try to obtain new polynuclear Cu(II) complexes with new topologies. By reaction of copper(II) methoxide, oximate ligands, tert-butylphosphonic acid and halides we have obtained four new triangular copper(II) compounds with the fragment {Cu3(μ-OH)-(oximate)3}2+ and formulae [Cu3(μ3-OH)(μ-Cl)(Py2CNO)3(tBuPO3H)]· 4H2O (1), [Cu3(μ3-OH)(μ-Br)(Py2CNO)3(tBuPO3H)]·3.5H2O (2), [Cu3(μ3-OH)(μ-Br)(PhPyCNO)3(tBuPO3H)(MeOH)]·1.5MeOH (3), [Cu3(μ3-OH)Cl2(PhPyCNO)3]·0.5H2O (4), (Py2CNO = di(2-pyridyl)-ketoximate, PhPyCNO = phenyl(2-pyridyl)ketoximate, tBuPO3H2 = tert-butylphosphonic acid). In three of the new trinuclear compounds (1–3) there is a tBuPO3H− ligand axially coordinated to one of the copper atoms and one Cl− or Br− ligand bridging the other two copper atoms. In the fourth complex the hydrogen phosphonate is not present and the Cl− ligand does not bridge two copper atoms but instead there are two terminal Cl− ligands. Compounds 1–3 show a known topology in copper oximato compounds: triangular systems with oximato bridging ligands containing a central μ3-hydroxo and two potentially chelating anions coordinated to the axial coordination sites of the copper atoms on opposite sides of the triangle's faces, one of them bridging two copper atoms and the other as terminal. These anions are usually carboxylate ligands.14,17,20,21 In the case of compounds 1–3 the terminal ligand is a hydrogenphosphonate that is stabilized by a hydrogen bond with the central μ3-hydroxo ligand and one Cl− or Br− ligand bridging the other two copper atoms on opposite sides. The other usual topology found in copper oximato chemistry is of dinuclear compounds with very strong antiferromagnetic coupling (−J around 500 cm−1).17,30

From the magnetic point of view, in a copper(II) equilateral triangle (Scheme 1), taking into account the isotropic Hamiltonian $\widehat{H} = -\sum_{ij} J_{ij}\hat{S}_i\,\hat{S}_j$, the derived equation for the magnetic susceptibility as a function of the temperature is

$$\chi_M = \frac{\mathrm{Ng}^2\beta^2 1+5\,\exp\,(\mathrm{x})}{4\kappa T\ \ 1+\exp\,(\mathrm{x})} \qquad (1)$$

where $x = 3J/2kT$. Using eqn (1) to fit the experimental magnetic susceptibility values measured in triangular copper(II) complexes, an obvious discrepancy is usually found mainly in the low-temperature magnetic data where the χMT value is smaller than that for one unpaired electron. This discrepancy arises mainly from the non-consideration in eqn (1), derived from the isotropic Hamiltonian, of the intramolecular antisymmetric exchange.22

Recently, F. Lloret and co-workers have published a new equation which includes the intramolecular antisymmetric exchange and the Zeeman interactions.22 This equation has been used to fit the experimental magnetic data of the new compounds 1–4.

Results and discussion

Synthesis

Previous attempts to prepare copper(II)/tert-butylphosphonate/oximate compounds without halide salts were unsuccessful. The structural determination of 1 in a few crystals formed in an attempt without halide salts but due to the existence of a little quantity of chloride impurities in the starting copper methoxide salt led us to attempt the synthesis by adding halide salts to the reaction mixture. The starting copper salt used was copper(II) methoxide to avoid another anion to be present in the reaction and also to generate a basic medium. The solvent used was methanol. The stoichiometric equation for compounds 1–4 is 1 Cu(II) methoxide + 1 oxime + 1 tertbutylphosphonic acid + 0.23 NaCl. Taking into account the formulae of compounds 1–3, the stoichiometric coefficient of NaCl was small compared to the required (0.33) to favour the tert-butylphosphonate as a ligand in the final compound.

Description of the structures of compounds 1 and 2

The structures of compounds 1 and 2 are very similar and differ mainly in the bridging halide, chlorine in 1 and bromine in 2, and in the number of lattice water molecules. In the description of the structures, the structural parameters of complex 2 will be discussed after those of complex 1.

The structures of compounds 1 and 2 consist of triangular [Cu3(μ3-OH)(μ-X)(Py2CNO)3(tBuPO3H)] units, X = Cl (1), Br (2) (Fig. 1 and 3), and lattice water molecules. Selected bond distances and angles are listed in Tables 1 and 2. The geometry around each of the copper(II) ions in the trimeric units is best described as a distorted square pyramid (τ = 0.046/0.053 for Cu1, 0.165/0.181 for Cu2 and 0.187/0.182 for Cu3, τ = Addison parameter, τ = 0 for an ideal square base pyramid and τ = 1 for an ideal trigonal bipyramid).31 Two of the copper ions (Cu1 and Cu3) have a NNOOX coordination environment, whereas the third copper ion (Cu2) has a NNOOO coordination environment. The trimeric skeleton is created by the oximato nitrogen atoms of one Py2CNO− ligand and the oxime oxygen atom of the adjacent Py2CNO− ligand, while the O atom of the μ3-OH− ligand (O1) completes the square-planar bases of the three metal atoms, with Cu1–O1, Cu2–O1, and Cu3–O1 bond distances of 1.947(4)/1.939(3), 1.931(3)/1.928(3), and 1.947(4)/1.944(3) Å, respectively. The bidentate halide ligand bridges Cu1 and Cu3, with Cu1–X1 and Cu3–X1 distances of 2.633(6)/ 2.855(1) and 2.684(5)/2.740(1) Å, respectively, while the oxygen of the monodentate tBuPO3H− ligand occupies the apical position of the Jahn–Teller-elongated square pyramid of Cu2, with a Cu2–O5 distance of 2.293(4)/2.276(4) Å.

The oximate bridges, Cu–N–O–Cu′, deviate slightly from planarity, with torsion angles of −3.1(4)°/−1.8(4)° (Cu1–N2–O2–Cu2), −17.7(6)°/−18.8(5)° (Cu2–N5–O3–Cu3), and −4.8(4)°/−4.9(4)° (Cu3–N8–O4–Cu1). The [Cu3] unit is strictly a scalene triangle in 1 and an isosceles triangle in 2, but can be considered in both cases as an isosceles triangle with Cu1⋯Cu2, Cu1⋯Cu3, and Cu2⋯Cu3 distances of 3.240/3.232, 3.042/3.042, and 3.229/3.232 Å, respectively. The oxygen atom of the hydroxo ligand, which is trapped in the metallacrown ring, lies at 0.638/0.625 Å out of the plane defined by the copper atoms.

There are intra- and intermolecular H-bonds. The capping μ3-OH hydrogen is engaged in a H-bond with an oxygen of the tert-butylphosphonate ligand [O1⋯O6 2.557(5)/2.546(4) Å; O1–H1A⋯O6 171(3)/167(3)°], whereas the other oxygen atom of the tert-butylphosphonate ligand makes intermolecular Hbonds with the tert-butylphosphonate ligand [O7⋯O6′ 2.600(4)/2.590(4) Å; O7–H7A⋯O6′ 177(6)/155.00°; −x, −y, 1 − z//1 − x, −y, 1 − z] of the other trinuclear unit, forming dimers of trimers not further connected (Fig. 2 and 4).

Description of the structure of compound 3

The structure of 3 consists of a triangular [Cu3(μ3-OH)(μ-Br)-(PhPyCNO)3(tBuPO3H)(MeOH)] unit (Fig. 5) and one and a half lattice methanol molecules. Selected bond distances and angles are listed in Table 3. The geometry around two of the copper(II) ions in the trimeric unit is best described as a distorted square pyramid (τ = 0.159 for Cu2 and 0.101 for Cu3).31 Cu2 has a NNOOO coordination environment, while Cu3 has a NNOOBr coordination environment. The third copper atom (Cu1) is hexacoordinated with a NNOOOBr coordination environment. The trimeric skeleton is created by the oximato nitrogen atoms of one PhPyCNO− ligand and the oxime oxygen atom of the adjacent PhPyCNO− ligand, whereas the O atom of the μ3-OH− ligand (O1) completes the square-planar bases of the three metal atoms, with Cu1–O1, Cu2–O1, and Cu3–O1 bond distances of 1.933(2), 1.948(2), and 1.967(3) Å, respectively. The bidentate bromide ligand bridges Cu1 and Cu3, with Cu1–Br1 and Cu3–Br1 distances of 3.123(1) and 2.726(1) Å, respectively, whereas the oxygen of the monodentate tBuPO3H− ligand occupies the apical position of the Jahn–Teller-elongated square pyramid of Cu2, with a Cu2–O5 distance of 2.316(3) Å. The sixth coordination position of Cu1 is occupied by an oxygen atom of a methanol ligand with a Cu1–O8 distance of 2.537(5) Å.

The oximate bridges, Cu–O–N–Cu′, deviate slightly from planarity, with torsion angles of −9.8(4)° (Cu1–O4–N6–Cu3), −11.0(4)° (Cu2–O2–N2–Cu1), and −18.0(4)° (Cu3–O3–N4–Cu2). The [Cu3] unit in 3 is strictly a scalene triangle but can be considered as an isosceles triangle with Cu1···Cu2, Cu1···Cu3, and Cu2···Cu3 distances of 3.218, 3.104, and 3.190 Å, respectively. The oxygen atom of the hydroxo ligand, which is trapped in the metallacrown ring, lies at 0.665 Å out of the plane defined by the copper atoms.

There are intra- and intermolecular H-bonds. The capping μ3-OH hydrogen is engaged in a H-bond with an oxygen of the tert-butylphosphonate ligand [O1···O7 2.642(4) Å; O1–H1A···O7 157(4)°], whereas the other oxygen atom of the tert-butylphosphonate ligand forms intermolecular H-bonds with another tert-butylphosphonate ligand [O6···O5′ 2.609(4) Å; O6–H6A···O5′ 172(6)°; −x, 1 − y, −z] forming dimers of trimers not further connected (Fig. 6). There is also a hydrogen bond involving the terminal methanol and the tert-butylphosphonate ligands [O8···O7 2.731(5) Å; O8–H8A···O7 174(7)°] (Fig. 6).

Description of the structure of compound 4

The structure of 4 consists of a triangular [Cu3(μ3-OH)-Cl2(PhPyCNO)3] unit (Fig. 7) and half of a lattice water molecule. Selected bond distances and angles are listed in Table 4. The geometry around two of the copper(II) ions in the trimeric unit is best described as a distorted square pyramid (τ = 0.006 for Cu1 and 0.223 for Cu3)31 with a NNOOCl coordination environment, while the third copper ion (Cu2) has a NNOO coordination environment. The trimeric skeleton is created by the oximato nitrogen atoms of one PhPyCNO− ligand and the oxime oxygen atom of the adjacent PhPyCNO− ligand, whereas the O atom of the μ3-OH− ligand (O1) completes the square-planar bases of the three metal atoms, with Cu1–O1, Cu2–O1, and Cu3–O1 bond distances of 1.986(2), 1.944(2), and 1.989(3) Å, respectively. The apical positions of Cu1 and Cu3 are occupied by two monodentate chloride ligands with Cu1–Cl1 and Cu3–Cl2 distances of 2.508(2) and 2.600(2) Å, respectively.

The oximate bridges, Cu–O–N–Cu′, deviate slightly from planarity, with torsion angles of 3.5(3)° (Cu1–O4–N6–Cu3), 32.7(3)° (Cu2–O2–N2–Cu1), and 17.7(3)° (Cu3–O3–N4–Cu2). The [Cu3] unit in 4 is strictly a scalene triangle but can be considered as an isosceles triangle with Cu1···Cu2, Cu1···Cu3, and Cu2···Cu3 distances of 3.207, 3.189, and 3.106 Å, respectively. The oxygen atom of the hydroxo ligand, which is trapped in the metallacrown ring, lies at 0.739 Å out of the plane defined by the copper atoms.

There is an intermolecular H-bond. The capping μ3-OH hydrogen is engaged in a H-bond with a chloride ligand [O1···Cl1 3.045(3) Å; O1–H1A···Cl1 170(4)°; −x, y, 1/2 − z] of other trinuclear unit, forming dimers of trimers not further connected (Fig. 8).

Magnetic properties

The magnetic properties of compounds 1–4 in the form of the χMT vs. T plot are shown in Fig. 9. At room temperature, the χMT values are in the range of 0.46–0.53 cm3 K mol−1 per trinuclear unit. These values are appreciably lower than those expected for three noninteracting S = 1/2 ions (χMT = 1.125 cm3 K mol−1, g = 2.0), suggesting very strong antiferromagnetic coupling. When the samples are cooled, χMT decreases continuously reaching values in the range of 0.26–0.34 cm3 K mol−1 at 2 K. These χMT vs. T curves clearly indicate strong intratrimer antiferromagnetic coupling. As the first approximation, it is often assumed that the three metal ions are structurally equivalent and the isotropic spin Hamiltonian $\widehat{H} = -\sum_{ij} J_{ij} \hat{S}_i \hat{S}_j$ can be used to describe the magnetic interactions using eqn (1). An attempt to use this approach, however, failed to reproduce the low-temperature decrease in the χMT vs. T plot for compounds 1–4. Different J and g values for the different magnetic centres do not improve the fit and lead to overparametrization.

The magnetic behaviour of the {Cu3(μ3-OH)} core has been extensively studied and S. Ferrer et al. have published a comprehensive review of the field.22 Taking into account this last paper, a new approach assuming the contribution of the antisymmetric exchange was considered. To fit the experimental data for compounds 1–4, we used the following Hamiltonian:

$$\widehat{H} = \widehat{H}_{iso} + \widehat{H}_{ASE} + \widehat{H}_{Zeem}$$

where Hiso is a Hamiltonian for isotropic exchange for an isosceles triangle with parameters J = J12 = J23 and j = J13; HASE is an axial Hamiltonian for the antisymmetric exchange with GZ parallel to the C3 axis and G⊥ = 0; HZeem is an axial Hamiltonian for the Zeeman interaction with gk = g1z = g2z = g3z and g⊥ = g1x = g2x = g3x = g1y = g2y = g3y. The exact analytical expression for the molar magnetic susceptibility as a function of the temperature can be found in ref. 22.

The best-fit parameters found in the fitting of the magnetic susceptibility experimental data for compounds 1–4 are listed in Table 5 and the theoretical curves calculated from these parameters are depicted as solid lines in Fig. 9.

Magnetostructural correlations

The more relevant structural parameters (bond lengths and angles) together with the exchange parameters for complexes 1–4 are listed in Table 6. These parameters are depicted in Scheme 2. The Cu–N,O and Cu–OH bond lengths (dCu–ox and dCu–OH, respectively) are the mean values for each compound. The β angle is defined by the average of the two most similar Cu–O–Cu angles within the triangle, whereas the γ angle refers to the most different one and the αav angle is defined as (2β + γ)/3. Finally, the values of the exchange parameters are as follows: J = J12 = J13, j = J23, and Jav = (2J + j)/3.

The magnetic interaction between two copper(II) ions within the triangle is mediated by both the diatomic N,O-(oxime) and monatomic O-(hydroxo) bridges. The structural parameters associated with the oxime bridge are comparable in the four compounds. The hydroxo bridge also presents similar Cu–

O distances (1.93–1.99 Å) in 1–4 and there is no relationship between this small variation and the values of the exchange coupling parameters. The magnetostructural correlation involves mainly the Cu–O–Cu bridgehead angle. In this respect, as observed in Table 6, the J_{av}, J, and j parameters depend on the α_{av}, β, and γ angles, respectively: the larger the angle, the larger the magnetic coupling. So, given that $\beta > \gamma$, then $|J| > |j|$, except for compound 4, for which $\gamma > \beta$ and $|j| > |J|$. It is worth noting that the Cu–O–Cu angle is directly related to the out-of-plane shift of the hydroxo bridge from the plane defined by the three copper atoms: the larger the shift, the smaller the angles. In fact, for similar compounds, it has been suggested that the more flattened the $Cu_3O(H)$ bridge (i.e. Cu–O–Cu angles closer to 120°), the stronger the magnetic interaction.[18] A plot of the Cu–O–Cu angle vs. the exchange coupling constant is shown in Fig. 10. The best linear fit is expressed by eqn (2), where J is given in cm^{-1}.

$$J = -19{:}080\theta + 1656 \qquad (2)$$

Eqn (2) is valid for compounds with the $\{Cu_3(\mu_3\text{-}OH)\text{-}(oximate)_3\}^{2+}$ fragment. Although the number of examples presented herein is hardly sufficient to establish a final accurate correlation, it may be concluded that the Cu–O–Cu bridgehead angle is one of the main factors governing the nature and magnitude of the magnetic coupling in the $\{Cu_3(\mu_3\text{-}OH)\text{-}(oximate)_3\}^{2+}$ triangular tricopper(II) complexes.

Experimental

Materials and physical measurements

All reagents, metal salts and ligands were used as obtained from Aldrich. Infrared spectra (4000–400 cm^{-1}) were recorded using KBr pellets on a Perkin-Elmer 380-B spectrophotometer. Magnetic susceptibility measurements under a magnetic field of 0.3 T in the temperature range 2–300 K and magnetization measurements in the field range of 0–5 T were performed with a Quantum Design MPMS-XL SQUID magnetometer at the Magnetic Measurements Unit of the University of Barcelona. All measurements were performed on polycrystalline samples. Pascal's constants were used to estimate the diamagnetic corrections, which were subtracted from the experimental susceptibilities to give the corrected molar magnetic susceptibilities.

Synthesis of [Cu3(μ3-OH)(μ-Cl)(Py2CNO)3(C4H9PO3H)]·4H2O (1)

All reagents, metal salts and ligands were used as obtained from Aldrich. To a solution of Cu(II) methoxide (0.201 g, 1.6 mmol) in methanol were added di-2-pyridyl ketone oxime (Py2CNOH, 0.319 g, 1.6 mmol), tert-butylphosphonic acid ($tBuPO_3H_2$, 0.221 g, 1.6 mmol) and NaCl (0.021 g, 0.36 mmol). After a few days of slow evaporation compound 1 was obtained as blue prism crystals. Anal.: Found: C, 42.6; H, 4.0; N, 12.0. Calcd for $C_{37}H_{43}ClCu_3N_9O_{11}P$: C, 42.5; H, 4.1; N, 12.0%. Selected IR data (KBr)/cm−1: 3423 (br), 2925 (m), 2854 (m), 1598 (s), 1529 (m), 1464 (s), 1437 (m), 1127 (vs), 1106 (m), 1054 (m), 898 (m).

Synthesis of [Cu3(μ3-OH)(μ-Br)(Py2CNO)3(C4H9PO3H)]·3.5H2O (2)

To a solution of Cu(II) methoxide (0.201 g, 1.6 mmol) in methanol were added di-2-pyridyl ketone oxime (Py2CNOH, 0.319 g, 1.6 mmol), tert-butylphosphonic acid (tBuPO3H2, 0.221 g, 1.6 mmol) and KBr (0.043 g, 0.36 mmol). After a few days of slow evaporation compound 1 was obtained as blue prism crystals. Anal.: Found: C, 41.0; H, 3.7; N, 12.0. Calcd for C37H43BrCu3N9O11P: C, 40.7; H, 4.0; N, 11.6%. Selected IR data (KBr)/cm−1: 3424 (br), 2960 (m), 2856 (m), 1598 (m), 1529 (m), 1464 (s), 1437 (m), 1127 (vs), 1105 (m), 1054 (m), 898 (m).

Synthesis of [Cu3(μ3-OH)(μ-Br)(PhPyCNO)3(C4H9PO3H)]·1.5MeOH (3)

To a solution of Cu(II) methoxide (0.201 g, 1.6 mmol) in methanol were added phenyl 2-pyridyl ketoxime (PhPyCNOH, 0.317 g, 1.6 mmol), tert-butylphosphonic acid (tBuPO3H2, 0.221 g, 1.6 mmol) and KBr (0.043 g, 0.36 mmol). After a few days of slow evaporation compound 1 was obtained as blue prism crystals. Anal.: Found: C, 46.0; H, 4.1; N, 8.0. Calcd for C41H42BrCu3N6O8P: C, 47.0; H, 4.0; N, 8.0%. Selected IR data (KBr)/cm−1: 3427 (br), 2852 (m), 1596 (s), 1528 (m), 1487 (m), 1463 (vs), 1441 (s), 1127 (s), 1106 (m), 1054 (m), 898 (m). Synthesis of [Cu3(μ3-OH)Cl2(PhPyCNO)3]·0.5H2O (4) To a solution of Cu(II) methoxide (0.201 g, 1.6 mmol) in methanol were added phenyl 2-pyridyl ketoxime (PhPyCNOH, 0.317 g, 1.6 mmol), tert-butylphosphonic acid (tBuPO3H2, 0.221 g, 1.6 mmol) and NaCl (0.021 g, 0.36 mmol). After a few days of slow evaporation compound 1 was obtained as blue prism crystals. Anal.: Found: C, 47.6; H, 3.4; N, 9.3. Calcd for C36H29Cl2Cu3N6O4.5: C, 49.2; H, 3.3; N, 9.6%. Selected IR data (KBr)/cm−1: 3399 (br), 1596 (m), 1489 (m), 1465 (vs), 1443 (m).

Crystallographic data collection and refinement

The X-ray single-crystal data of compound 1 were collected on a Bruker X8 Kappa APEX-II diffractometer with a graphitemonochromator utilizing Mo-Kα radiation (λ = 0.71073 Å), with ω and φ-scans at 100(1) K.32 X-ray data of compound 2 were collected on a Bruker CCD SMART1000 diffractometer with a graphite-monochromator utilizing Mo-Kα radiation (λ = 0.71073 Å), with ω and φ-scans at 100(1) K33 and those of compounds 3 and 4 were collected on a MAR345 diffractometer with an image plate detector and φ-scans at 110(2) K. The crystallographic data, conditions retained for the intensity data collection and some features of the structure refinements are listed in Table 7. Data processing, including Lorentz-polarization and absorption corrections, was performed using the SADABS34 computer programs. The structure was solved by direct methods and refined by full-matrix least-squares methods, using the SHELXTL program package.35 All nonhydrogen atoms were refined anisotropically. The H atoms attached to C and N atoms were added theoretically and treated as riding on the concerned parent atoms. H atoms attached to O atoms were located from difference Fourier maps and included in the final refinement cycles on fixed positions.

Conclusions

Four new trinuclear copper(II) complexes with the fragment $\{Cu_3(\mu_3\text{-}OH)(oximate)_3\}^{2+}$ (1–4) were prepared from 2-pyridyl ketoxime derivatives and structurally characterized by X-ray crystallography. Their magnetic data have been analyzed using an isotropic and antisymmetric exchange Hamiltonian. All these compounds show strong antiferromagnetic and antisymmetric exchange. The magnetostructural study presented here has shown a lineal correlation for complexes with the fragment $\{Cu_3(\mu_3\text{-}OH)(oximate)_3\}^{2+}$ between the Cu–O–Cu angle and the isotropic exchange parameters (J and j).

Acknowledgements

This research was supported by the Spanish Ministerio de Educación y Ciencia (MEC) (Grant CTQ2012-30662) and the Generalitat de Catalunya (Grant 2009SGR1454). We thank the Unidade de Raios X-RIAIDT, University of Santiago de Compostela, Spain, for performing intensity measurements of complexes 1 and 2.

References

1 P. Chaudhuri, Coord. Chem. Rev., 2003, 243, 143.

2 C. J. Milios, C. P. Raptopoulou, A. Terzis, F. Lloret, R. Vicente, S. P. Perlepes and A. Escuer, Angew. Chem., Int. Ed., 2004, 116, 212.

3 C. J. Milios, C. P. Raptopoulou, A. Terzis, F. Lloret, R. Vicente, S. P. Perlepes and A. Escuer, Angew. Chem., Int. Ed., 2004, 43, 210.

4 C. J. Milios, E. Kefalloniti, C. P. Raptopoulou, A. Terzis, R. Vicente, N. Lalioti, A. Escuer and S. P. Perlepes, Chem. Commun., 2003, 819.

5 C. J. Milios, T. C. Stamatatos, P. Kyritsis, A. Terzis, C. P. Raptopoulou, R. Vicente, A. Escuer and S. P. Perlepes, Eur. J. Inorg. Chem., 2004, 2885.

6 R. Clérac, H. Miyasaka, M. Yamashita and C. Coulon, J. Am. Chem. Soc., 2002, 124, 12837.

7 C. J. Milios, T. C. Stamatatos and S. P. Perlepes, Polyhedron, 2006, 25, 134.

8 A. Chakraborty, K. L. Gurunatha, A. Muthulakshmi, S. Dutta, S. K. Pati and T. K. Maji, Dalton Trans., 2012, 41, 5879.

9 T. Afrati, C. M. Zaleski, C. Dendrinou-Samara, G. Mezel, J. W. Kampf, V. L. Pecoraro and D. P. Kessissoglou, Dalton Trans., 2007, 2658.

10 M. Wenzel, R. S. Forgan, A. Faure, K. Mason, P. A. Tasker, S. Piligkos, E. K. Brechin and P. G. Plieger, Eur. J. Inorg. Chem., 2009, 4613.

11 R. Beckett and B. F. Hoskins, J. Chem. Soc., Dalton Trans. 1972, 291.

12 Y.-B. Jiang, H.-Z. Kou, R.-J. Wang, A.-L. Cui and J. Ribas, Inorg. Chem., 2005, 44, 709.

13 T. Afrati, C. Dendrinou-Samara, C. Raptopoulou, A. Terzis, V. Tangoulis and D. P. Kessissoglou, Dalton Trans., 2007, 5156.

14 T. Afrati, C. Dendrinou-Samara, C. Raptopoulou, A. Terzis, V. Tangoulis and D. P. Kessissoglou, Inorg. Chem., 2008, 47, 7545.

15 P. F. Ross, R. K. Murmann and E. O. Schlemper, Acta Crystallogr., Sect. B: Struct. Crystallogr. Cryst. Chem., 1974, 30, 1120.

16 G.-X. Liu, W. Guo, S. Nishihara and X.-M. Ren, Inorg. Chim. Acta, 2011, 368, 165.

17 A. Escuer, B. Cordero, M. Font-Bardia and T. Calvet, Inorg. Chem., 2010, 49, 9752.

18 R. J. Butcher, C. J. O’Connor and E. Sinn, Inorg. Chem., 1981, 20, 537.

19 Y. Agnus, R. Louis, B. Metz, C. Boudon, J. P. Gisselbrecht and M. Gross, Inorg. Chem., 1991, 30, 3155.

20 T. C. Stamatatos, J. C. Vlahopoulou, Y. Sanakis, C. P. Raptopoulou, V. Psycharis, A. K. Boudalis and S. P. Perlepes, Inorg. Chem. Commun., 2006, 9, 814.

21 T. Afrati, A. A. Pantazaki, C. Dendrinou-Samara, C. Raptopoulou, A. Terzis and D. P. Kessissoglou, Dalton Trans., 2010, 39, 765.

22 S. Ferrer, F. Lloret, E. Pardo, J. M. Clemente-Juan, M. Liu-Gonzalez and S. Garcia-Granda, Inorg. Chem., 2012, 51, 985, and references cited therein.

23 N. F. Curtis, O. P. Gladkikh, S. L. Heath and K. R. Morgan, Aust. J. Chem., 2000, 53, 577.

24 P. Chakrabarti, V. G. Puranik, J. P. Naskar, S. Hati and D. Datta, Indian J. Chem., Sect. A: Inorg., Bio-inorg., Phys., Theor. Anal. Chem., 2000, 39, 571.

25 S. Ferrer, E. Aznar, F. Lloret, A. Castiñeiras, M. Liu-González and J. Borrás, Inorg. Chem., 2007, 46, 372.

26 M. Wenzel, R. S. Forgan, A. Faure, K. Mason, P. A. Tasker, S. Piligkos, E. K. Brechin and P. G. Plieger, Eur. J. Inorg. Chem., 2009, 4613.

27 D. Maity, P. Mukherjee, A. Ghosh, M. G. B. Drew, C. Diaz and G. Mukhopadhyay, Eur. J. Inorg. Chem., 2010, 807. 28 S. Karmakar, O. Das, S. Ghosh, E. Zangrando, M. Johann, E. Rentschler, T. Weyhermüller, S. Khanra and T. K. Paine, Dalton Trans., 2010, 39, 10920.

29 V. Chandrasekhar, T. Senapati, A. Dey and S. Hossain, Dalton Trans., 2011, 40, 5394.

30 E. S. Koumousi, C. P. Raptopuolou, S. P. Perlepes, A. Escuer and T. C. Stamatatos, Polyhedron, 2010, 29, 204, and references therein.

31 A. W. Addison, T. N. Rao, J. Reedijk, J. V. Rijjin and G. C. Verschoor, J. Chem. Soc., Dalton Trans., 1984, 1349.

32 Bruker Analytical X-ray Systems, Version 2009-3.0, APEX2: Bruker AXS Inc., 2009.

33 Bruker Analytical X-ray Systems, SMART: Bruker Molecular Analysis Research Tool, Version 5.054, 1997–98.

34 G. M. Sheldrick, SADABS, v. 2, University of Göttingen, Germany, 2001.

35 G. M. Sheldrick, Acta Crystallogr., Sect. A: Fundam. Crystallogr., 2008, 64, 112.

Legends to figures

Figure 1. Structure of compound 1. Colour code: Cu(II) = light blue; N = dark blue; O = red; P = orange; Cl = green; C = grey. Hydrogen atoms have been omitted for clarity.

Figure 2. Dimer of trimers formed by H-bonds of compound 1.

Figure 3. Structure of compound 2. Colour code: Cu(II) = light blue; N = dark blue; O = red; P = orange; Br = purple; C = grey. Hydrogen atoms have been omitted for clarity.

Figure 4. Dimer of trimers formed by H-bonds of compound 2.

Figure 5. Structure of compound 3. Colour code: Cu(II) = light blue; N = dark blue; O = red; P = orange; Br = purple; C = grey. Hydrogen atoms have been omitted for clarity.

Figure 6. Dimer of trimers formed by H-bonds of compound 3.

Figure 7. Structure of compound 4. Colour code: Cu(II) = light blue; N = dark blue; O = red; Cl = green; C = grey. Hydrogen atoms have been omitted for clarity.

Figure 8. Dimer of trimers formed by H-bonds of compound 4.

Figure 9. χMT vs. T plot in the 300–2 K range of temperatures for complexes 1–4. The solid lines are the best fit (see text).

Scheme 2 The angle β is defined by the average of the most similar Cu–OH–Cu angles within the triangle, whereas the angle γ refers to the most different one of them. The angle α is defined as the average of the three Cu–OH–Cu angles of the complex.

Figure 10. Plot of the Cu–O–Cu angle vs. the exchange coupling constant.

Table 1 Bond distances and angles of compound 1

Bond distances (Å)							
Cu1–Cl1	2.633(6)	Cu1–O1	1.947(4)	Cu1–O2	2.928(3)	Cu1–O4	1.947(3)
Cu1–N1	1.974(4)	Cu1–N2	1.976(4)	Cu2–O1	1.931(3)	Cu2–O2	1.945(4)
Cu2–O3	2.927(4)	Cu2–O5	2.293(4)	Cu2–N4	1.950(3)	Cu2–N5	1.983(5)
Cu3–Cl1	2.684(5)	Cu3–O1	1.947(4)	Cu3–O3	1.920(4)	Cu3–O4	2.896(3)
Cu3–N7	1.963(4)	Cu3–N8	1.963(4)				
Bond angles (°)							
Cl1–Cu1–O1	80.97(16)	Cl1–Cu1–O2	92.19(13)	Cl1–Cu1–O4	91.63(16)	Cl1–Cu1–N1	112.63(17)
Cl1–Cu1–N2	101.32(16)	O1–Cu1–O2	66.75(13)	O1–Cu1–O4	92.60(15)	O1–Cu1–N1	164.15(17)
O1–Cu1–N2	88.09(16)	O2–Cu1–O4	158.09(14)	O2–Cu1–N1	103.38(15)	O4–Cu1–N1	95.00(17)
O4–Cu1–N2	166.97(15)	N1–Cu1–N2	81.40(16)	O1–Cu2–O2	92.69(15)	O1–Cu2–O3	67.32(13)
O1–Cu2–O5	94.04(14)	O1–Cu2–N4	170.45(17)	O1–Cu2–N5	89.62(18)	O2–Cu2–O3	152.52(15)
O2–Cu2–O5	94.02(15)	O2–Cu2–N4	94.84(15)	O2–Cu2–N5	160.48(19)	O3–Cu2–O5	105.59(14)
O3–Cu2–N4	103.60(13)	O5–Cu2–N4	91.30(14)	O5–Cu2–N5	105.16(18)	N4–Cu2–N5	81.33(18)
Cl1–Cu3–O1	79.64(18)	Cl1–Cu3–O3	103.94(17)	Cl1–Cu3–O4	72.89(12)	Cl1–Cu3–N7	117.54(18)
Cl1–Cu3–N8	85.91(16)	O1–Cu3–O3	93.53(16)	O1–Cu3–O4	67.86(12)	O1–Cu3–N7	158.84(14)
O1–Cu3–N8	88.74(15)	O3–Cu3–O4	161.37(15)	O3–Cu3–N7	93.90(16)	O3–Cu3–N8	170.13(19)
O4–Cu3–N7	103.87(12)	N7–Cu3–N8	80.80(15)	Cu1–O1–Cu3	102.76(18)	Cu2–O1–Cu3	112.77(17)
Cu1–O1–Cu2	113.32(19)						

Table 2 Bond distances and angles of compound 2

Bond distances (Å)							
Br1–Cu1	2.855(1)	Br1–Cu3	2.740(1)	Cu1–O1	1.939(3)	Cu1–O2	2.927(3)
Cu1–O4	1.938(3)	Cu1–N1	1.977(4)	Cu1–N2	1.970(4)	Cu2–O1	1.928(3)
Cu2–O2	1.949(4)	Cu2–O3	2.932(4)	Cu2–O5	2.276(4)	Cu2–N4	1.946(3)
Cu2–N5	1.956(5)	Cu3–O1	1.944(3)	Cu3–O3	1.935(3)	Cu3–O4	2.888(3)
Cu3–N7	1.982(4)	Cu3–N8	1.967(3)				
Bond angles (°)							
Cu1–Br1–Cu3	65.84(2)	Br1–Cu1–O1	79.24(8)	Br1–Cu1–O2	90.50(7)	Br1–Cu1–O4	92.84(9)
Br1–Cu1–N1	115.06(11)	Br1–Cu1–N2	100.28(10)	O1–Cu1–O2	67.06(10)	O1–Cu1–O4	92.46(12)
O1–Cu1–N1	163.53(14)	O1–Cu1–N2	88.25(14)	O2–Cu1–O4	158.24(10)	O2–Cu1–N1	103.22(12)
O4–Cu1–N1	94.80(13)	O4–Cu1–N2	166.76(13)	N1–Cu1–N2	81.34(15)	O1–Cu2–O2	92.97(12)
O1–Cu2–O3	67.33(10)	O1–Cu2–O5	93.83(11)	O1–Cu2–N4	170.98(17)	O1–Cu2–N5	89.75(16)
O2–Cu2–O3	152.94(12)	O2–Cu2–O5	94.17(14)	O2–Cu2–N4	94.42(16)	O2–Cu2–N5	160.26(18)
O3–Cu2–O5	105.09(13)	O3–Cu2–N4	103.98(16)	O5–Cu2–N4	90.80(15)	O5–Cu2–N5	105.16(18)
N4–Cu2–N5	81.6(2)	Br1–Cu3–O1	82.20(8)	Br1–Cu3–O3	100.43(11)	Br1–Cu3–O4	77.60(6)
Br1–Cu3–N7	116.24(12)	Br1–Cu3–N8	90.07(11)	O1–Cu3–O3	93.28(14)	O1–Cu3–O4	67.56(10)
O1–Cu3–N7	158.49(15)	O1–Cu3–N8	88.75(14)	O3–Cu3–O4	160.83(14)	O3–Cu3–N7	93.97(17)
O3–Cu3–N8	169.49(16)	O4–Cu3–N7	104.05(14)	N7–Cu3–N8	80.67(17)	Cu1–O1–Cu2	113.45(13)
Cu1–O1–Cu3	103.18(13)	Cu2–O1–Cu3	113.19(13)				

Table 3 Bond distances and angles of compound 3

Bond distances (Å)							
Br1–Cu1	3.123(1)	Br1–Cu3	2.726(1)	Cu1–O1	1.933(2)	Cu1–O2	2.917(3)
Cu1–O4	1.947(3)	Cu1–O8	2.537(5)	Cu1–N1	1.977(3)	Cu1–N2	1.975(3)
Cu2–O1	1.948(2)	Cu2–O2	1.956(3)	Cu2–O3	2.932(3)	Cu2–O5	2.316(3)
Cu2–N3	1.970(3)	Cu2–N4	1.977(3)	Cu3–O1	1.967(3)	Cu3–O3	1.933(3)
Cu3–O4	2.903(3)	Cu3–N5	1.981(3)	Cu3–N6	1.974(3)		
Bond angles (°)							
Cu1–Br1–Cu3	63.67(3)	Br1–Cu1–O1	74.80(9)	Br1–Cu1–O2	81.35(6)	Br1–Cu1–O4	89.06(9)
Br1–Cu1–O8	161.43(10)	Br1–Cu1–N1	107.55(11)	Br1–Cu1–N2	87.75(9)	O1–Cu1–O2	69.46(9)
O1–Cu1–O4	92.80(10)	O1–Cu1–O8	86.98(13)	O1–Cu1–N1	172.66(11)	O1–Cu1–N2	91.34(11)
O2–Cu1–O4	161.49(9)	O2–Cu1–O8	89.06(11)	O2–Cu1–N1	103.77(10)	O4–Cu1–O8	95.45(13)
O4–Cu1–N1	94.19(11)	O4–Cu1–N2	173.93(13)	O8–Cu1–N1	90.12(14)	O8–Cu1–N2	89.20(13)
N1–Cu1–N2	81.87(12)	O1–Cu2–O2	94.99(10)	O1–Cu2–O3	67.63(9)	O1–Cu2–O5	93.01(11)
O1–Cu2–N3	170.53(11)	O1–Cu2–N4	89.64(12)	O2–Cu2–O3	153.48(10)	O2–Cu2–O5	96.07(12)
O2–Cu2–N3	94.30(11)	O2–Cu2–N4	160.95(14)	O3–Cu2–O5	104.41(9)	O3–Cu2–N3	103.01(10)
O5–Cu2–N3	87.86(13)	O5–Cu2–N4	102.15(12)	N3–Cu2–N4	80.96(12)	Br1–Cu3–O1	84.77(8)
Br1–Cu3–O3	101.57(8)	Br1–Cu3–O4	80.86(6)	Br1–Cu3–N5	108.03(10)	Br1–Cu3–N6	89.37(9)
O1–Cu3–O3	93.30(10)	O1–Cu3–O4	67.32(9)	O1–Cu3–N5	162.89(13)	O1–Cu3–N6	88.64(11)
O3–Cu3–O4	160.32(10)	O3–Cu3–N5	95.09(12)	O3–Cu3–N6	169.02(12)	O4–Cu3–N5	102.77(11)
N5–Cu3–N6	80.40(13)	Cu1–O1–Cu2	112.01(11)	Cu1–O1–Cu3	105.47(12)	Cu2–O1–Cu3	109.13(12)

Table 4 Bond distances and angles of compound 4

Bond distances (Å)							
Cu1–Cl1	2.508(2)	Cu1–O1	1.986(2)	Cu1–O2	2.929(3)	Cu1–O4	1.948(3)
Cu1–N1	2.012(3)	Cu1–N2	1.993(3)	Cu2–Cl2	3.019(2)	Cu2–O1	1.944(2)
Cu2–O2	1.935(3)	Cu2–O3	2.910(3)	Cu2–N3	1.978(3)	Cu2–N4	1.973(3)
Cu3–Cl2	2.600(2)	Cu3–O1	1.989(3)	Cu3–O3	1.951(3)	Cu3–O4	2.899(3)
Cu3–N5	1.995(4)	Cu3–N6	1.971(3)				
Bond angles (°)							
Cl1–Cu1–O1	98.52(8)	Cl1–Cu1–O2	98.91(7)	Cl1–Cu1–O4	95.37(9)	Cl1–Cu1–N1	93.53(11)
Cl1–Cu1–N2	99.23(10)	O1–Cu1–O2	66.65(9)	O1–Cu1–O4	94.30(11)	O1–Cu1–N1	164.80(12)
O1–Cu1–N2	88.95(11)	O2–Cu1–O4	157.62(10)	O2–Cu1–N1	102.44(11)	O4–Cu1–N1	93.75(12)
O4–Cu1–N2	164.40(13)	N1–Cu1–N2	79.96(13)	Cl2–Cu2–O1	72.50(8)	Cl2–Cu2–O2	101.69(9)
Cl2–Cu2–O3	69.52(6)	Cl2–Cu2–N3	106.40(11)	Cl2–Cu2–N4	79.58(10)	O1–Cu2–O2	92.99(10)
O1–Cu2–O3	69.52(9)	O1–Cu2–N3	173.26(13)	O1–Cu2–N4	92.45(12)	O2–Cu2–O3	161.95(8)
O2–Cu2–N3	93.75(12)	O2–Cu2–N4	174.55(12)	O3–Cu2–N3	103.79(11)	N3–Cu2–N4	80.82(14)
Cl2–Cu3–O1	82.47(8)	Cl2–Cu3–O3	94.91(8)	Cl2–Cu3–O4	80.87(6)	Cl2–Cu3–N5	115.53(10)
Cl2–Cu3–N6	90.17(9)	O1–Cu3–O3	93.88(11)	O1–Cu3–O4	69.49(9)	O1–Cu3–N5	160.04(12)
O1–Cu3–N6	90.96(12)	O3–Cu3–O4	163.19(10)	O3–Cu3–N5	93.07(12)	O3–Cu3–N6	173.40(12)
O4–Cu3–N5	103.46(11)	N5–Cu3–N6	80.91(13)	Cu1–O1–Cu2	109.38(11)	Cu1–O1–Cu3	106.68(11)
Cu2–O1–Cu3	104.32(12)						

Table 5 Best-fit magnetic parameters for 1–4

Complex	$-J_{av}$	θ	δ	G	$g_{\parallel}$	$g_{\perp}$
1	448	−0.12	176	62	2.26	2.01
2	451	−0.14	158	73	2.29	2.10
3	422	−0.16	176	62	2.35	2.06
4	385	−0.34	82	47	2.22	2.13

Table 6 Magnetostructural data for 1–4[a]

Complex	$-J_{av}$	α	$-J$	β	$-j$	γ	d_{Cu-ox}	d_{Cu-OH}
1	448	109.7	507	113.1	331	102.8	1.956	1.941
2	451	110.0	503	113.4	345	103.4	1.952	1.935
3	422	109.0	480	110.7	304	105.6	1.961	1.948
4	385	106.8	331	105.5	413	109.4	1.962	1.973

[a] The parameters are defined in Scheme 2. The distances and bond angles are average values.

Table 7 Crystal data and structure refinement for complexes 1–4

	1	2	3	4
Formula	$C_{37}H_{43}ClCu_3N_9O_{11}P$	$C_{74}H_{84}Br_2Cu_6N_{18}O_{21}P_2$	$C_{170}H_{192}Br_4Cu_{12}N_{24}O_{38}P_4$	$C_{144}H_{116}Cl_8Cu_{12}N_{24}O_{18}$
Weight	1046.84	2164.59	4385.48	3516.69
Crystal system	Triclinic	Triclinic	Monoclinic	Monoclinic
Space group	$P\bar{1}$	$P\bar{1}$	$C2/c$	$C2/c$
a (Å)	12.4303(4)	12.302(3)	34.556(13)	28.805(11)
b (Å)	13.4622(5)	13.355(3)	12.953(5)	10.739(4)
c (Å)	15.7280(8)	15.779(5)	23.542(4)	27.103(6)
α (°)	106.861(3)	109.133(4)	90	90
β (°)	96.972(3)	95.518(4)	104.03(2)	109.63(2)
γ (°)	113.633(2)	113.774(3)	90	90
V (Å^3)	2184.0(2)	2161.8(1)	10223(6)	7897(5)
Z	2	1	2	2
ρ_{calc} (g cm^{-3})	1.592	1.663	1.425	1.479
F(000)	1070	1096	4464	3552
μ (mm^{-1})	1.613	2.490	2.105	1.782
T (K)	100.0(1)	100.0(1)	293(2)	293(2)
R^a [$I > 2\sigma(I)$]	0.0489	0.0418	0.0573	0.0577
wR^b [$I > 2\sigma(I)$]	0.1108	0.1014	0.1652	0.1495
S^c	1.047	1.002	1.067	1.072

$^a R = \sum(|F_o| - |F_c|)/\sum|F_o|$. $^b wR = [\sum w(|F_o| - |F_c|)^2/\sum w|F_o|^2]^{1/2}$. $^c \sum = [\sum w(|F_o| - |F_c|^2)/(N_o - N_p)]^{1/2}$.

Scheme 1

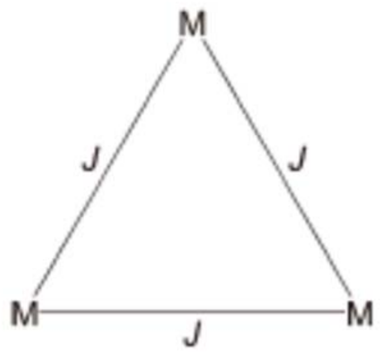

Figure 1

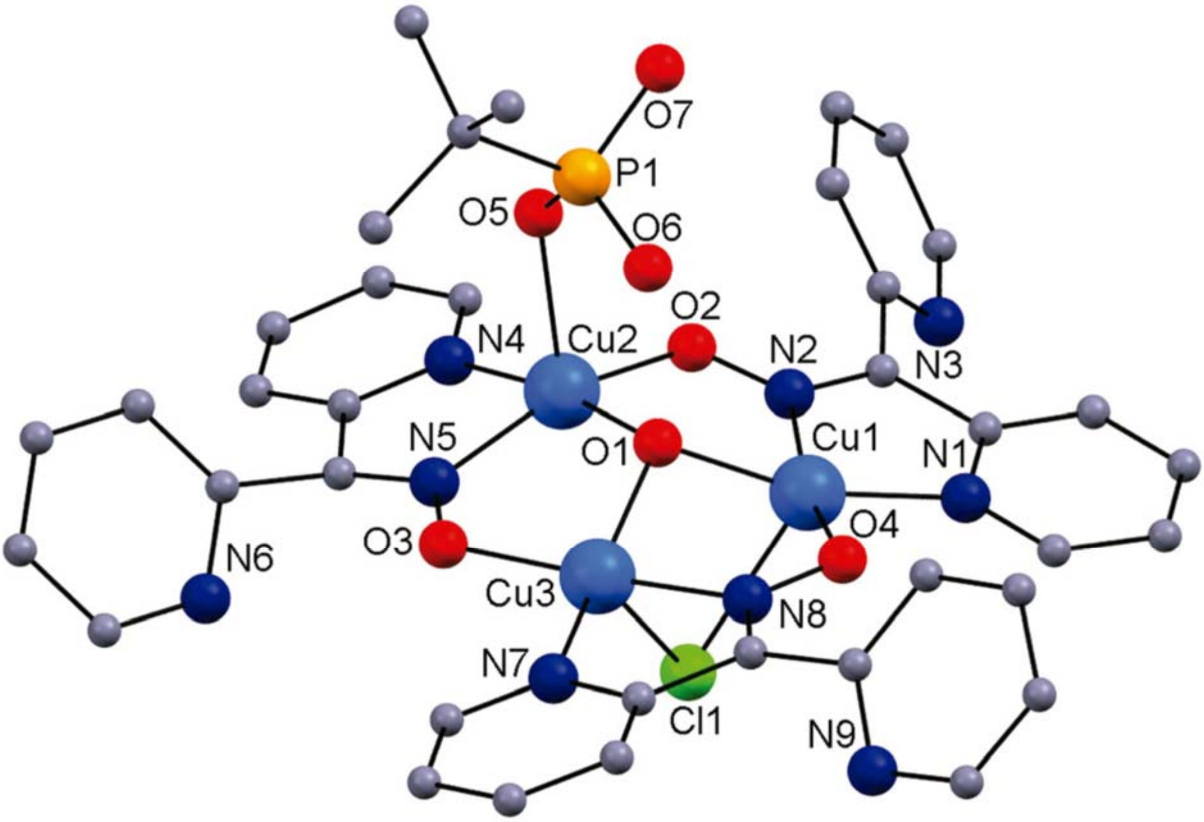

Figure 2

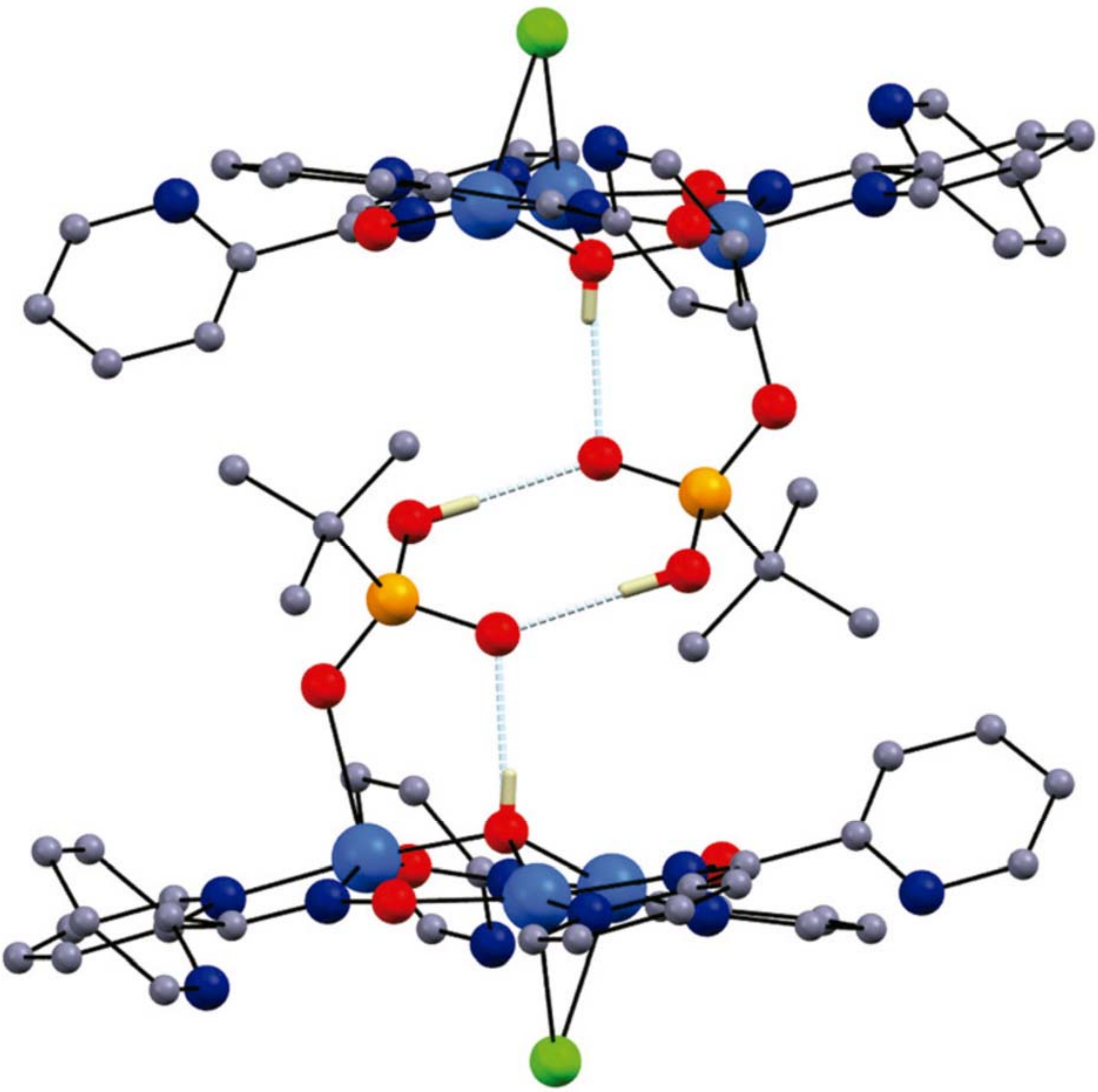

Figure 3

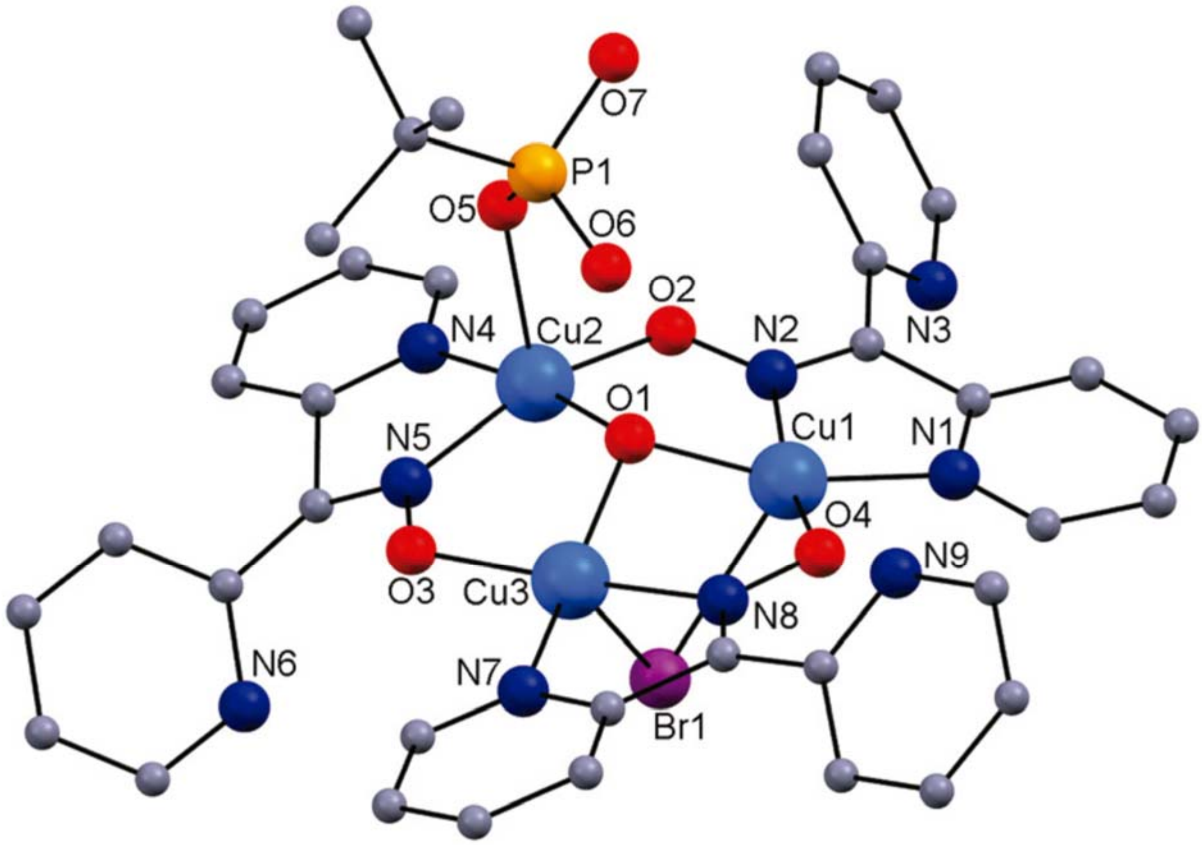

Figure 4

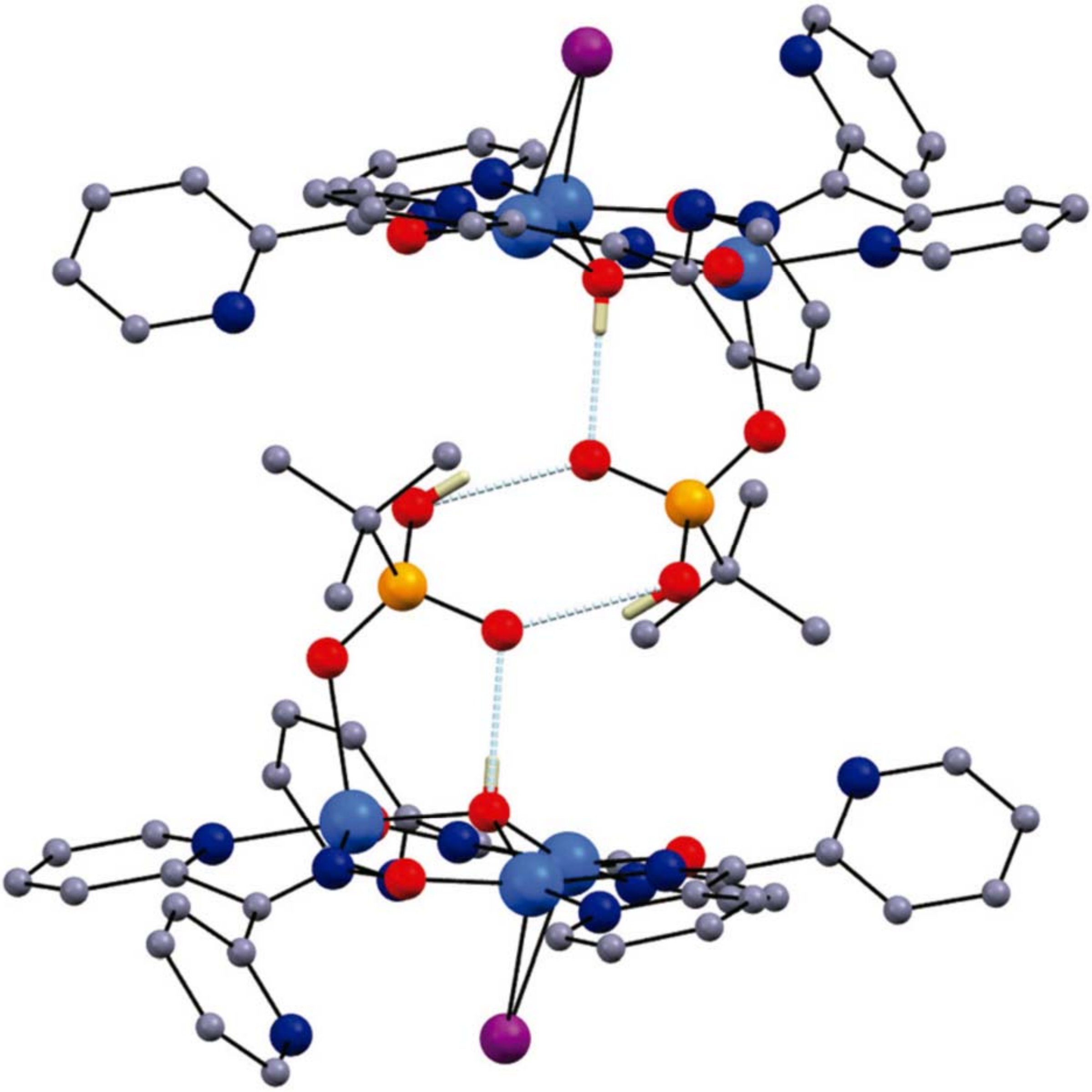

Figure 5

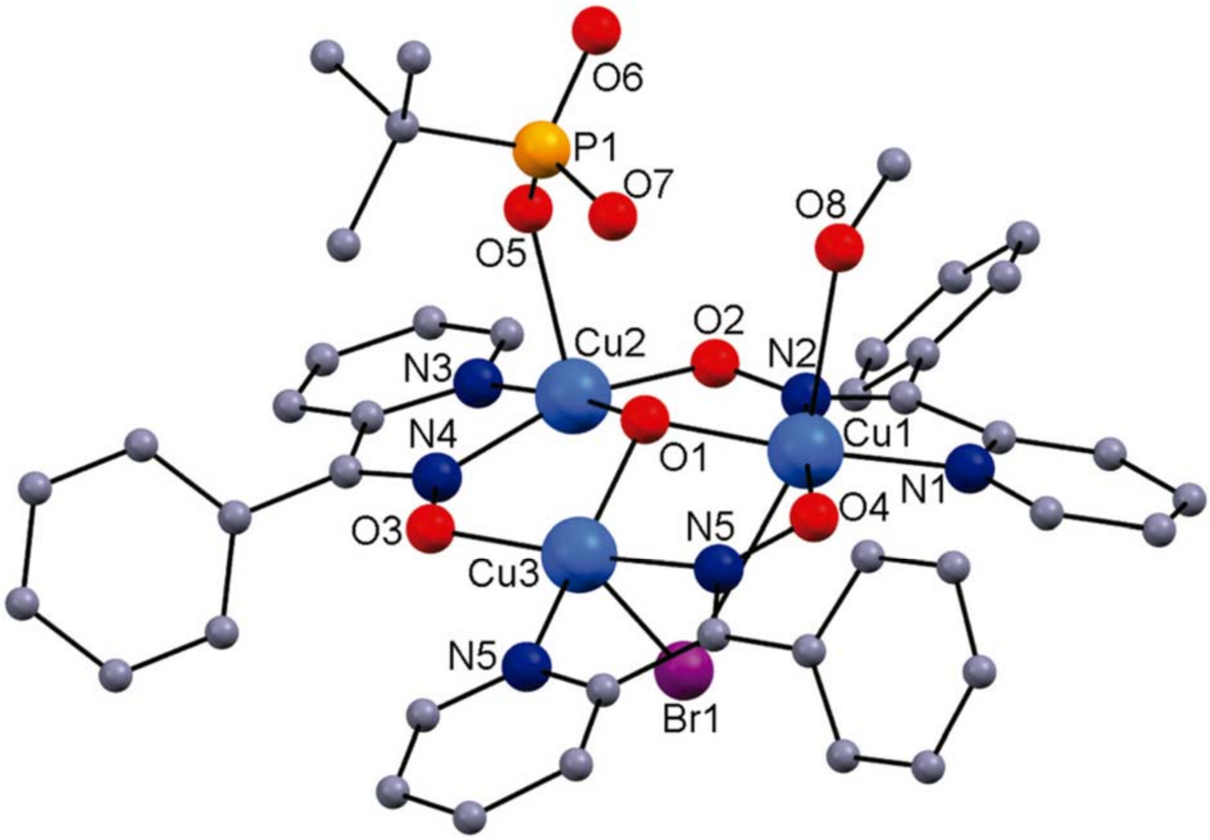

Figure 6

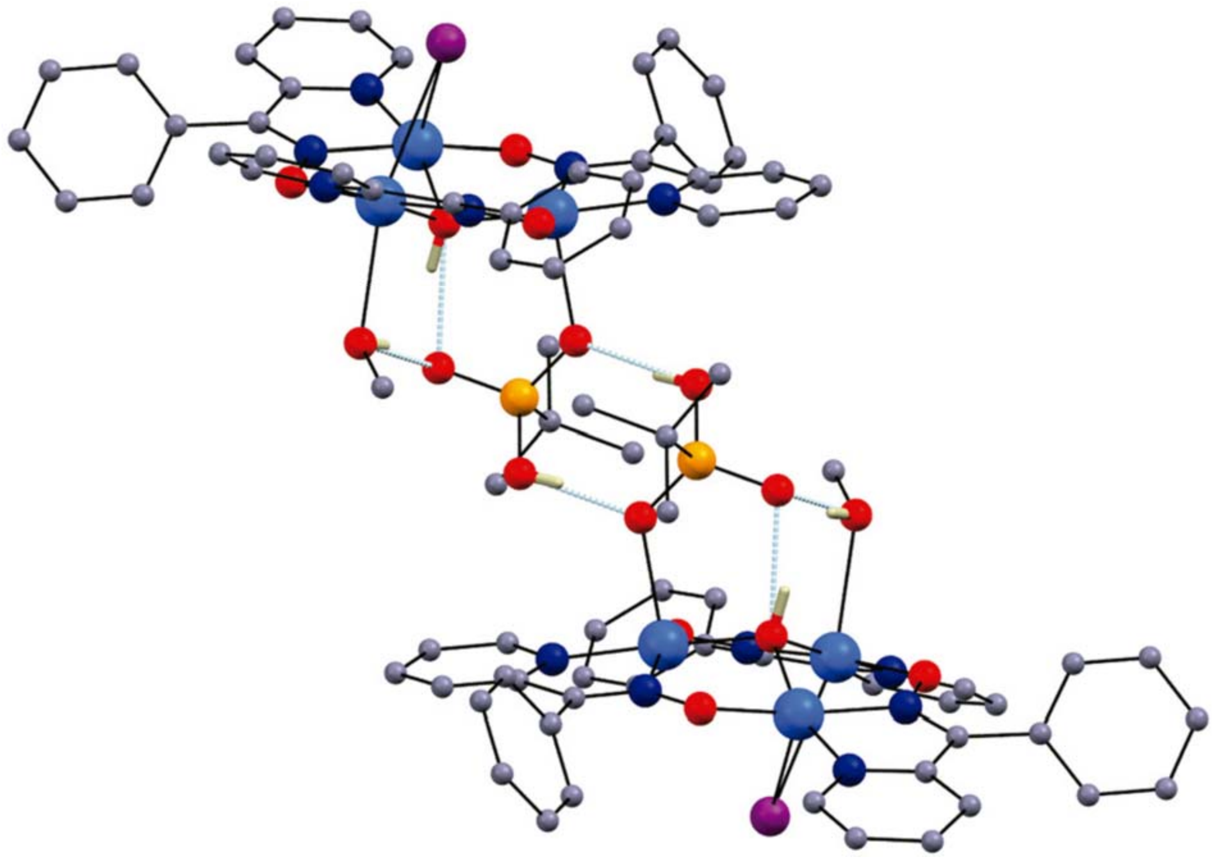

Figure 7

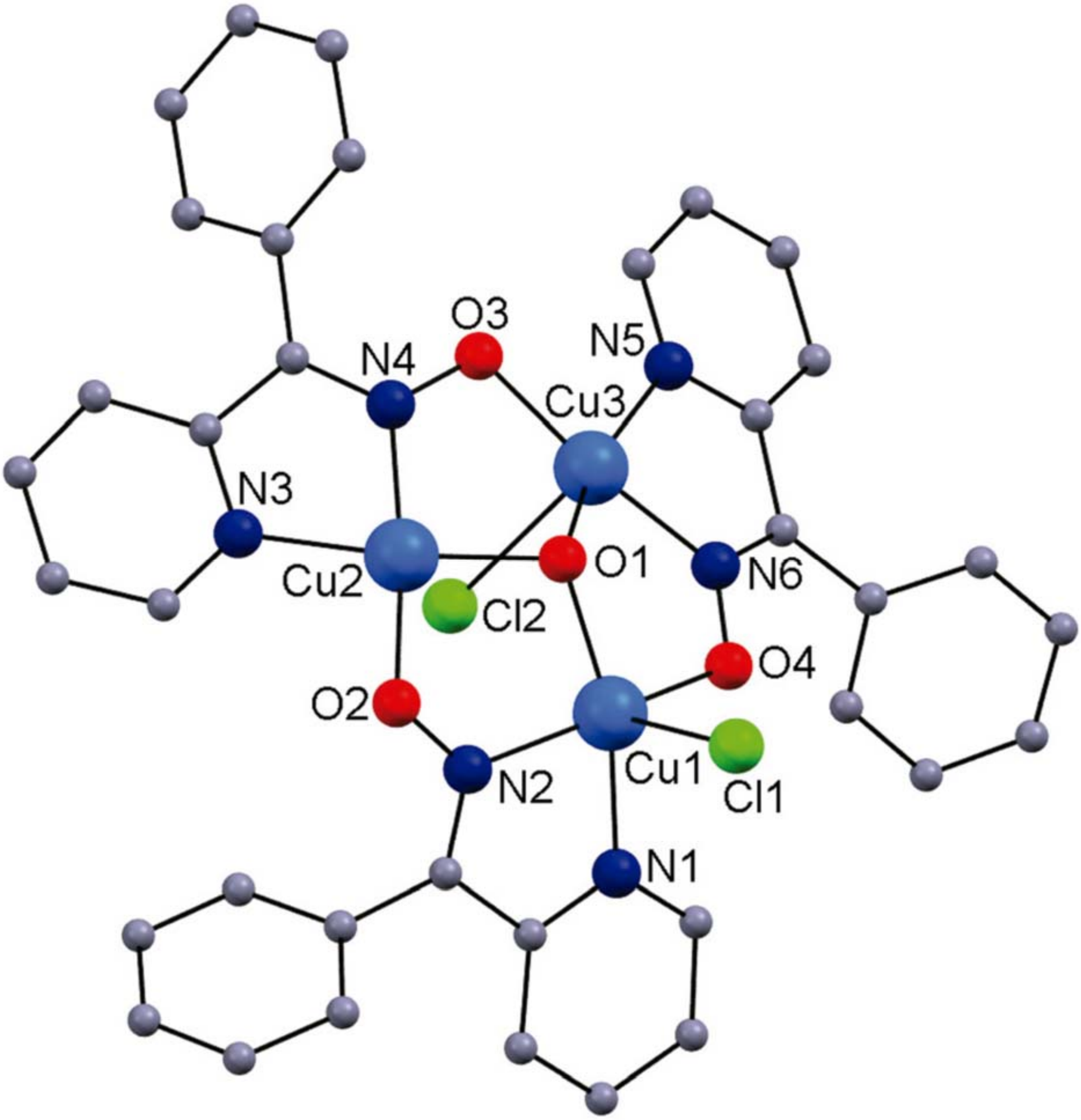

Figure 8

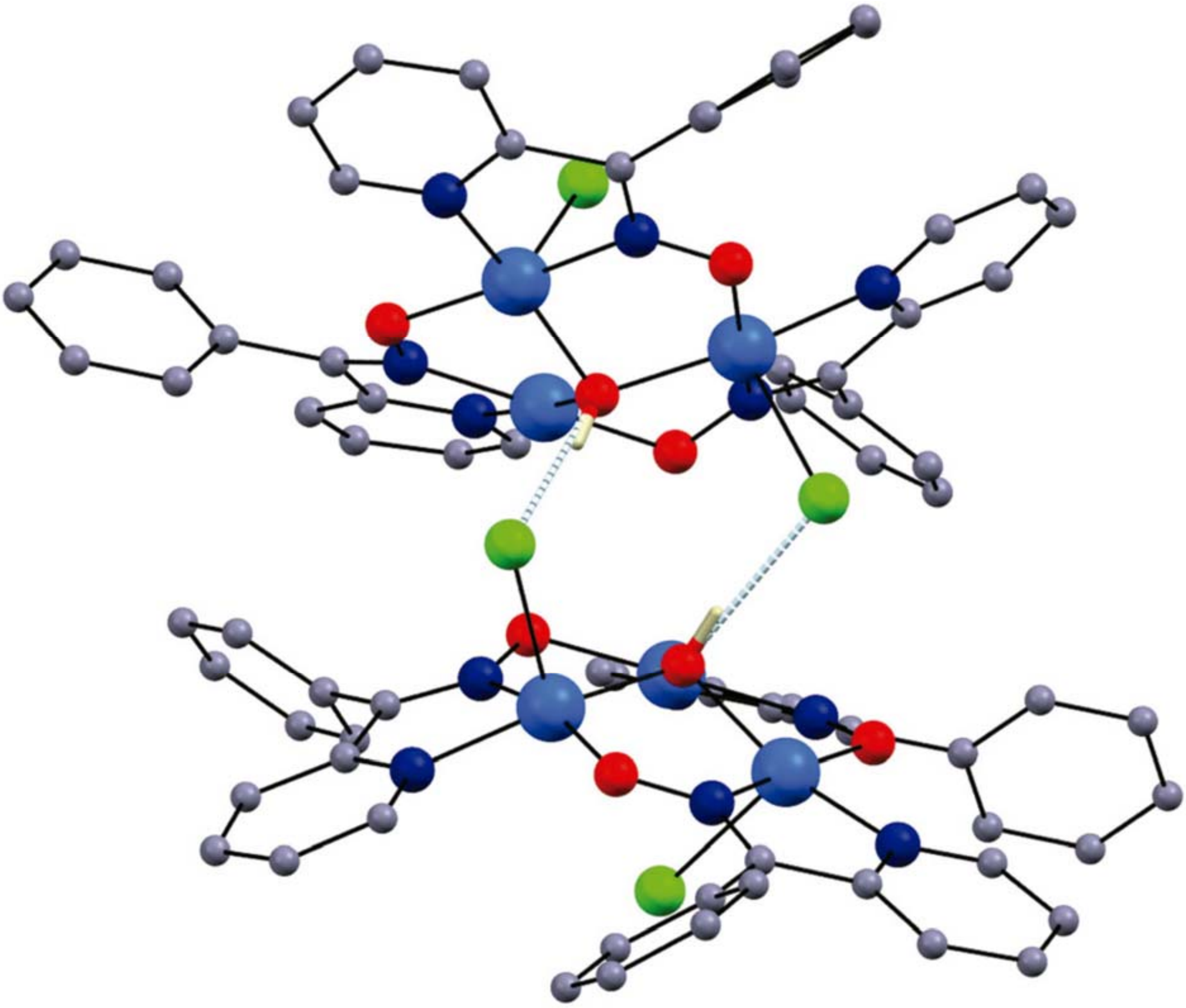

Figure 9

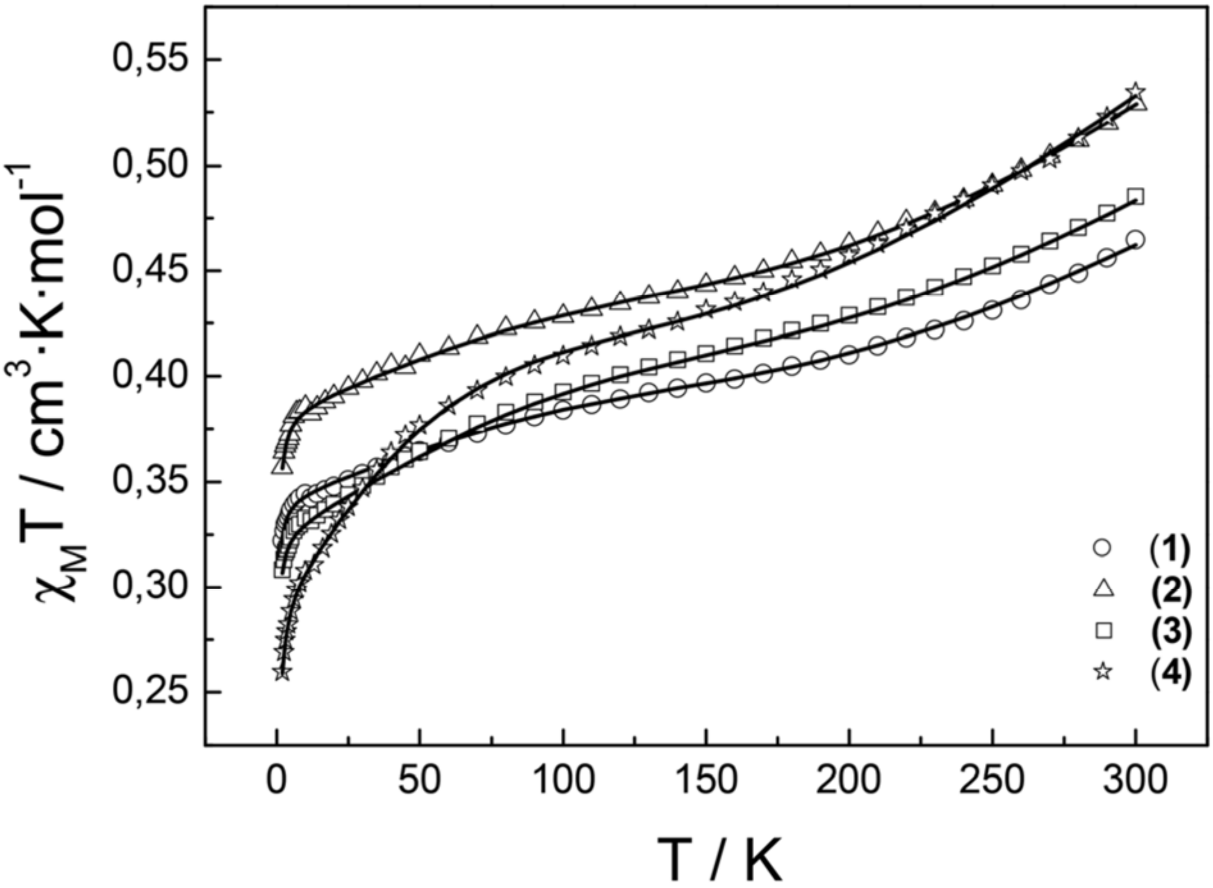
0,55
0,50
0,45
0,40
0,35
0,30
0,25
$\chi_M T$ / cm^3·K·mol^{-1}
0
50
100
150
200
250
300
T / K
(1)
(2)
(3)
(4)

Scheme 2

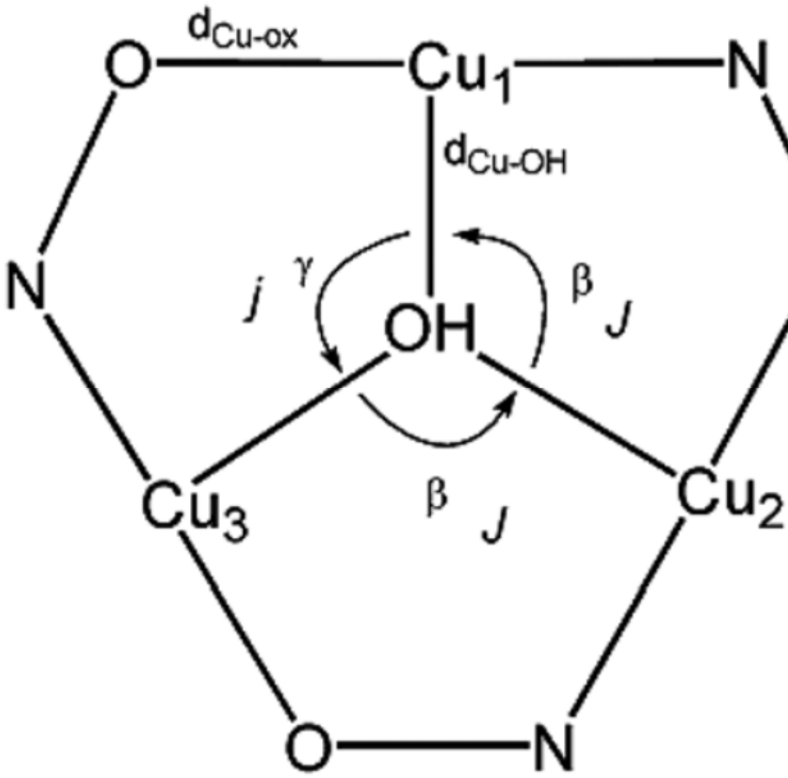

Figure 10